

APPLICATION OF TOPOLOGICAL DERIVATIVE TO THE OPTIMAL DESIGN OF THREE-DIMENSIONAL STRUCTURAL ARRANGEMENTS OF FLAT PLATES

Augusto Romero^{a,b}, Sebastián M. Giusti^{a,b} and Javier E. Salomone^a

^a*Grupo de Investigación y Desarrollo en Mecánica Aplicada, Universidad Tecnológica Nacional - Facultad Regional Córdoba (UTN-FRC), Maestro M. López y Cruz Roja Argentina, 5000 Ciudad de Córdoba, Provincia de Córdoba, Argentina, {aromero,sgiusti,jsalomone}@frc.utn.edu.ar, <https://www.investigacion.frc.utn.edu.ar/gidma/>*

^b*Consejo Nacional de Investigaciones Científicas y Técnicas (CONICET)*

Keywords: Folded structures, Structural optimization, Topological optimization.

Abstract. This work addresses the problem of optimal topological design of three-dimensional structures composed of plate arrays based on the use of topological derivatives. These structural arrays consist of planar elements linked at their edges. Their modeling is performed by coupling a membrane model and a bending-plate model. The geometric and material representation is accomplished using level-set curves. To minimize a cost function, the topological derivative value is used to guide the evolution of the level-set curve. A theoretical framework and case studies of academic and industrial applications are presented.

1 INTRODUCTION

Shell structures are very common in several engineering sectors including civil, industrial, nuclear, and marine. In civil engineering, these structures are used in roofs, domes, bridges, walls and silos. The key factors are economic mass production and lightweight. A thin shell is stiff against in-plane forces and easily deformed against out-of-plane bending. Such thin shell structures must be properly designed to avoid large deflections while effectively supporting the prescribed loads, which is difficult to achieve using only intuitive or empirical methods. For problems with such challenges, structural optimization can be a powerful method for a wide range of problems. A simpler approach is to consider such structures as a sequence of folded plates. For this particular case, the membrane and bending effects are decoupled in the middle surface that defines the plate.

The mathematical model of folded plates is given by a system of linear equations of elliptic type. Hence, it can be shown by the standard procedure of the speed method (Sokołowski and Zolésio, 1992) that the elliptic boundary value problem under consideration is well posed from the point of view of shape optimization.

In particular, it means that by the elliptic regularity of the weak solutions to the model, the existence of the shape and material derivatives is ensured. This fact implies the existence of the shape gradient for the boundary shape functional. Therefore, the classical shape optimization method by boundary variations can be applied to the numerical solution of the shape optimization problem. We are interested, however, in modern approaches to shape-topological optimization, i.e., we want to admit a broader family of admissible domains obtained by non-smooth perturbations of regular domains. In other words, we perform the asymptotic analysis of solutions to the state equation in the singularly perturbed geometrical domains. The non-smooth domain perturbations can be analyzed only in the framework of asymptotic analysis (Novotny and Sokołowski, 2013) because such perturbations cannot be described by bilipschitzian mappings of the speed method. The singular perturbations include the insertion of holes or cavities into the reference domain. It is known (Novotny and Sokołowski, 2013) that the holes or cavities can be considered as the limit case of inclusions for the limit passage of the so-called contrast parameters. For numerical solutions to optimum design problems, it is useful to insert inclusions made of a different material characterized by a contrast parameter for the elastic property.

The starting point of the numerical procedure for structural optimum design is the numerical evaluation of the topological derivative. Since the topological derivative formula is obtained at the continuous level, to use this information to identify local minima or maxima in a numerical optimization procedure we need the discrete values of the topological derivative. The precision of the numerical evaluation of topological derivatives should be sufficient for such an identification procedure. In the case of minimization problems, the negative part of the level-set function associated with the topological derivative evaluated in the reference domain is selected. Therefore, it only needs to look for the local minima of the topological derivative for one isolated circular inclusion $B_\varepsilon(\hat{x})$, for all $\hat{x} \in \Omega$. Let us recall that the topological derivative for one circular inclusion $B_\varepsilon \mapsto J_\varepsilon(\Omega)$ is a function $\hat{x} \mapsto \mathcal{T}(\hat{x})$ defined in Ω such that the following asymptotic expansion holds for $\varepsilon \rightarrow 0$,

$$J_\varepsilon(\Omega) = J(\Omega) + f(\varepsilon)\mathcal{T}(\hat{x}) + o(f(\varepsilon)). \quad (1)$$

The function $f(\varepsilon)$, such that $f(\varepsilon) \rightarrow 0^+$ with $\varepsilon \rightarrow 0^+$, can be specified from the asymptotic analysis concerning the small parameter $\varepsilon \rightarrow 0$.

The insertion of one inclusion results in perturbations of the coefficients of the elliptic operators. For one inclusion, we perform the sensitivity analysis of the perturbed coupled equations concerning the small parameter $\varepsilon \rightarrow 0$. Such an analysis gives rise to $\varepsilon > 0$ of the shape gradient of the specific shape functional $\varepsilon \mapsto J_\varepsilon(\Omega)$. By the limit transition $\varepsilon \rightarrow 0^+$ the topological derivative of the functional is obtained as a function of the point $\hat{x} \in \Omega$. This means that for fixed ε there are known two expansions of the cost $\varepsilon \mapsto j(\varepsilon) := J_\varepsilon(\Omega)$, with respect to the small parameters $\delta \rightarrow 0$ and $\varepsilon \rightarrow 0^+$, respectively

- for $\varepsilon > 0$,

$$j(\varepsilon + \delta) = j(\varepsilon) + \delta j'(\varepsilon) + O(\delta^2), \tag{2}$$

- for $\varepsilon = 0^+$,

$$j(\varepsilon) = j(0) + f(\varepsilon)\mathcal{T}(\hat{x}) + o(f(\varepsilon)). \tag{3}$$

By $j'(\varepsilon)$ denotes the classical shape derivative of the cost functional $J_\varepsilon(\Omega)$ for the shape perturbations of the boundary of inclusion $B_\varepsilon(\hat{x})$. The second formula of asymptotic type is established for the radius $\varepsilon = 0^+$ of the inclusion. Therefore, we are going to determine the unknown function

$$\hat{x} \mapsto \mathcal{T}(\hat{x}), \tag{4}$$

by the method of asymptotic analysis. We recall (Zochowski, 1988) that there is a relation between the two formulas (2) and (3), namely:

$$\mathcal{T}(\hat{x}) = \lim_{\varepsilon \rightarrow 0^+} \frac{j'(\varepsilon)}{f'(\varepsilon)}. \tag{5}$$

The optimal shell design problem using topological derivative remains open, being a topic of deep scientific, technological, and industrial interest due to the various areas of engineering in which it is necessary to apply it. However, many advances have been achieved on the optimal plate design problem by using topological derivatives. The topological derivatives associated with thin and thick plate models have been obtained in Amstutz (2010) and Sales et al. (2015) respectively. Their implementation for the optimal design of mono and multi-material structures has been carried out in Carvalho et al. (2021) and Romero and Giusti (2020), while in Romero (2022) they have been used for the design of bi-material thick and thin plate mechanisms.

2 OPTIMIZATION PROBLEM

2.1 Topological derivative

Let us now introduce the optimization problem, given by:

$$\min_{\chi} \mathcal{J}(\chi, u, w) = \mathcal{J}_m(\chi, u) + \mathcal{J}_b(\chi, w), \tag{6}$$

where $\mathcal{J}(\chi, u, w)$ is the shape functional to be minimized, and depends on the characteristic function χ , the in-plane elastic displacement u and the out-of-plane displacement w . Note that in the definition of $\mathcal{J}(\chi, u, w)$ the membrane and bending effects in the structural domain Ω are uncoupled. For this work, we consider the total potential energy of the system, given by:

$$\mathcal{J}_m(\chi, u) = -\frac{1}{2} \int_{\Omega} \sigma_{\chi}(u) \cdot \nabla^s u - \int_{\Omega} \bar{b} \cdot u + \int_{\Gamma_t} \bar{t} \cdot u, \quad \text{and} \tag{7}$$

$$\mathcal{J}_b(\chi, w) = -\frac{1}{2} \int_{\Omega} M_{\chi}(w) \cdot \nabla \nabla w - \int_{\Omega} \bar{g} \cdot w - \int_{\Gamma_q} \bar{q} w + \int_{\Gamma_m} \bar{m} \partial_n w + \sum_{i=1}^{ns} \bar{Q}_i w(x_i). \tag{8}$$

The displacement field u is determined within linear elasticity as: Find $u \in \mathcal{U}$ such that:

$$\int_{\Omega} \sigma_{\chi}(u) \cdot \nabla^s \eta_u = \int_{\Omega} \bar{b} \cdot \eta_u + \int_{\Gamma_t} \bar{t} \cdot \eta_u \quad \forall \eta_u \in \mathcal{V}_u \quad (9)$$

where $\sigma_{\chi}(u) = \mathbb{C}_{\chi} \nabla^s u$ is the elastic stress tensor, \mathbb{C}_{χ} is the fourth-order elasticity tensor and ∇^s is that symmetric part of the gradient operator ∇ . For the case of isotropic materials, the constitutive elastic tensor can be written as:

$$\mathbb{C} = \frac{E}{1 - \nu^2} ((1 - \nu)\mathbb{I} + \nu I \otimes I), \quad (10)$$

being \mathbb{I} and I the fourth- and second-order identity tensors, respectively, E the Young modulus and ν the Poisson ratio. The optimization procedure is based on representing the domain in a bi-material fashion. The topology is identified by the strong material distribution (denoted as Ω^h) and the inclusions of weak material (denoted as Ω^s) are used to mimic the holes. The constitutive properties of these regions are characterized by the elasticity tensor \mathbb{C}_{χ} and the contrast parameter γ . Based on that, we have

$$\mathbb{C}_{\chi} = \begin{cases} \mathbb{C} & \forall x \in \Omega^h \\ \gamma \mathbb{C} & \forall x \in \Omega^s \end{cases} \quad (11)$$

In the problem presented in (9), \mathcal{U} and \mathcal{V}_u are the appropriate set and functional space, respectively, accounting for the Dirichlet boundary condition and its variations.

The transversal displacement field w is determined within the Kirchhoff plate-bending problem given by: Find $w \in \mathcal{W}$ such that:

$$- \int_{\Omega} M_{\chi}(w) \cdot \nabla \nabla \eta_w = \int_{\Omega} \bar{g} \eta_w + \int_{\Gamma_q} \bar{q} \eta_w - \int_{\Gamma_m} \bar{m} \partial_n \eta_w - \sum_{i=1}^{ns} \bar{Q}_i \eta(x_i). \quad \forall \eta_w \in \mathcal{V}_w \quad (12)$$

where $M_{\chi}(w) = -\frac{h^3}{12} \mathbb{C}_{\chi} \nabla \nabla w$ is the elastic moment tensor, being h the thickness of the plate. As before, in the above equation, \mathcal{W} and \mathcal{V}_w are the appropriate set and functional space, respectively, accounting for the Dirichlet boundary condition and its variations. In problems (9) and (12) the symbols $\bar{b}, \bar{t}, \bar{g}, \bar{q}, \bar{m}$ and \bar{Q}_i are used to denote the set of admissible loads for the considered structural models, see [Campeão et al. \(2014\)](#).

Since the structural domain is characterized by planes linked in some of its linear edges, the kinematics of the elastic membrane and plate inside of the domain Ω remain uncoupled. Therefore, the sensitivity of each problem (membrane and bending) to the topological changes can be measured separately. Based on this fact, the topological derivative of functional $\mathcal{J}(\chi, u, w)$ in (6) can be written as:

$$\mathcal{TJ}_{\chi}(\hat{x}) = \mathcal{TJ}_m(\hat{x}) + \mathcal{TJ}_b(\hat{x}), \quad (13)$$

where the topological derivatives of the membrane and bending effects are

$$\mathcal{TJ}_m(\hat{x}) = \mathbb{P}_m \sigma(u)(\hat{x}) \cdot \nabla^s u(\hat{x}), \quad \text{and} \quad \mathcal{TJ}_b(\hat{x}) = \mathbb{P}_b M(w)(\hat{x}) \cdot \nabla \nabla w(\hat{x}), \quad (14)$$

being $\sigma(u)(\hat{x})$ and $M(w)(\hat{x})$ the stress and moment tensor evaluated at point \hat{x} . In the same manner, $\nabla^s u(\hat{x})$ and $\nabla \nabla w(\hat{x})$ are the strain and curvature tensor at point \hat{x} . The fourth-order polarization tensors \mathbb{P}_m and \mathbb{P}_b in (14) are given by:

$$\mathbb{P}_m = \frac{1}{2} \frac{1 - \gamma}{1 + \beta_m \gamma} \left((1 + \beta_m) \mathbb{I} + \frac{1}{2} (\alpha - \beta_m) \frac{1 - \gamma}{1 + \alpha \gamma} I \otimes I \right), \quad \text{and} \quad (15)$$

$$\mathbb{P}_b = \frac{1}{2} \frac{1 - \gamma}{1 + \beta_b \gamma} \left(\frac{4\beta_b}{1 - \nu} \mathbb{I} + \alpha \beta_b \frac{1 + 3\nu}{1 - \nu^2} \frac{1 - \gamma}{1 + \alpha \gamma} I \otimes I \right), \quad (16)$$

with $\alpha = \frac{1+\nu}{1-\nu}$, $\beta_m = \frac{3-\nu}{1+\nu}$ and $\beta_b = \frac{1-\nu}{3+\nu}$. We refer the readers interested in developing the above expressions to the work by [Novotny and Sokołowski \(2013\)](#).

2.2 Optimization procedure

By considering the level-set domain representation, the strong (or hard) material is characterized by a function $\Psi \in L^2(\Omega)$ such that

$$\Omega^h = \{x \in \Omega, \Psi(x) < 0\} , \tag{17}$$

whereas the weak (or soft) material domain is defined by

$$\Omega^s = \{x \in \Omega, \Psi(x) > 0\} . \tag{18}$$

Now, let us consider the topological derivative $\mathcal{T}\mathcal{J}_\chi(\hat{x})$. According to [Amstutz and André \(2006\)](#), a sufficient condition of *local optimality* of problem (6) for the class of perturbations consisting of circular inclusions is

$$\mathcal{T}\mathcal{J}_\chi(x) > 0 \quad \forall x \in \Omega . \tag{19}$$

To devise a level-set-based algorithm whose aim is to produce a topology that satisfies (19) it is convenient to define the function

$$g(x) = \begin{cases} -\mathcal{T}\mathcal{J}_\chi^h(x) & \text{if } x \in \Omega^h \\ \mathcal{T}\mathcal{J}_\chi^s(x) & \text{if } x \in \Omega^s \end{cases} . \tag{20}$$

With the above definition and (17,18) it can be easily established that the sufficient condition (19) is satisfied if the following equivalence relation between the functions g and the level-set Ψ holds

$$\exists \tau > 0 \quad \text{s.t} \quad g = \tau \Psi , \tag{21}$$

or, equivalently,

$$\theta := \arccos \left[\frac{\langle g, \Psi \rangle_{L^2(\Omega)}}{\|g\|_{L^2(\Omega)} \|\Psi\|_{L^2(\Omega)}} \right] = 0 , \tag{22}$$

where θ is the angle between the vectors g and Ψ in $L^2(\Omega)$. Starting from a given level-set function $\Psi_0 \in L^2(\Omega)$ which defines the chosen initial guess for the optimum topology, the algorithm proposed by [Amstutz and André \(2006\)](#) produces a sequence $(\Psi_i)_{i \in N}$ of level-set functions that provides successive approximations to the sufficient condition for optimality (21). The sequence satisfies

$$\begin{aligned} \Psi_0 &\in L^2(\Omega) , \\ \Psi_{i+1} &\in \text{co}(\Psi_i, g_i) \quad \forall i \in N , \end{aligned} \tag{23}$$

where $\text{co}(\Psi_i, g_i)$ is the convex hull of $\{\Psi_i, g_i\}$. In the current algorithm the initial guess Ψ_0 is normalized. With \mathcal{S} denoting the unit sphere in $L^2(\Omega)$, the algorithm is explicitly given by

$$\begin{aligned} \Psi_0 &\in \mathcal{S} , \\ \Psi_{i+1} &= \frac{1}{\sin \theta_i} \left[\sin((1 - \kappa_i)\theta_i)\Psi_i + \sin(\kappa_i\theta_i)\frac{g_i}{\|g_i\|_{L^2(\Omega)}} \right] , \end{aligned} \tag{24}$$

where $\kappa_i \in [0, 1]$ is a step size determined by a line search to decrease the value of the cost functional \mathcal{J}_χ . The iterative process is stopped when for some iteration the obtained decrease in

\mathcal{J}_χ is smaller than a given numerical tolerance. If, at this stage, the optimality condition (21,22) is not satisfied to the desired degree of accuracy, i.e. if $\theta_{i+1} > \epsilon_\theta$, where ϵ_θ is a pre-specified convergence tolerance, then a uniform mesh refinement of the structure is carried out and the procedure is continued.

Based on the above description, the main steps of the algorithm can be summarized as follows:

1. Choose an initial level-set function by defining the initial guess for the optimal structure domain.
2. Define the domains Ω^h and Ω^s according to (17) and (18).
3. Define the constitutive properties in each discrete domain Ω^h and Ω^s according to (11).
4. Obtain the discretized fields u and w by solving, respectively, the problems (9) and (12) by using a standard numerical procedure.
5. Compute the discrete topological derivative field (13).
6. Obtain the function $g(x)$ according to (20) by using the discrete values of the topological derivative and compute the θ angle with (22).
7. Update the level-set function Ψ_{i+1} according to (24) and update the domains Ω^h and Ω^s by considering (17) and (18).
8. Check convergence $\theta_{i+1} \leq \epsilon_\theta$. If True: Exit. If False: goto 3.

3 NUMERICAL EXAMPLES

To illustrate the applicability of expression (13) and the optimization procedure presented in the previous Section, we present two numerical examples. To numerically solve the membrane and bending state equations (9) and (12), respectively, a standard FEM was used. For the bending problem the DKT finite element [Batoz \(1982\)](#) was implemented. And for the membrane problem, the ANDES finite element [Felippa and Militello \(1992\)](#); [Felippa \(2003\)](#) was selected and implemented. The coupling of the displacements u and w was made in the sides belonging to two or more planes by considering proper rotations of the global DOF into local ones in the triangle. The full stiffness matrix, in the triangle element local domain, is represented as diagonal by blocks. The local DOF at the nodes in each formulation of finite elements are presented in Fig. 1. The global DOF in a finite element mesh is shown in Fig. 2. Finally, by considering a volume constraint in the optimization problem, we can avoid a trivial solution to the problem (6).

3.1 Example 1. Structural tube optimal design

This example considers the structural optimization of a tube with a square cross-section. The aspect ratio of the tube is 1 : 1 : 5, thus the length of the tube is 5 times the side of the square. The four sides are clamped at one end of the tube, and four unitary forces are considered on the opposite sides. These forces are in the direction of the side (at its midpoint) and aligned to produce a torsional effect in the tube. The geometry of the tube and the boundary conditions are shown in Fig. 3, and the obtained result in Fig. 4.

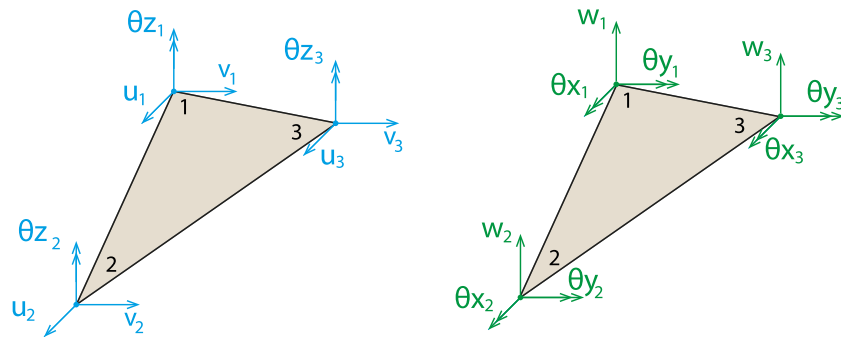


Figure 1: Finite elements: membrane-ANDES (left) and bending-DKT (right)

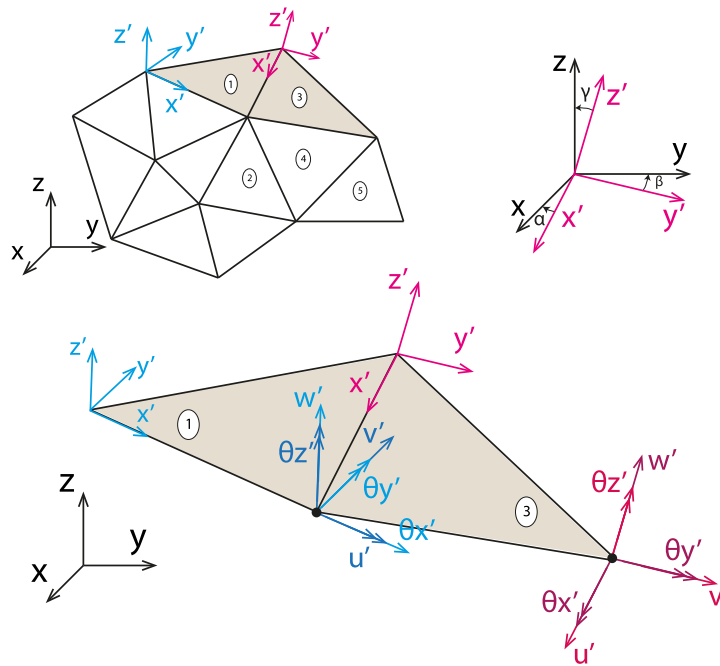


Figure 2: Coupling DOF in finite elements mesh

3.2 Example 2. Structural beam optimal design

This example considers the structural optimization of a beam with a square cross-section. The aspect ratio of the beam geometry is 1 : 1 : 2. The domain was constructed by considering an array of $19 \times 9 \times 9$ structural plates. All sides of the plates are clamped at one end of the beam, and one unitary force is considered on the center of the opposite sides. In this example, we explore the possibility of study a solid domain made by regular arrangements of plates. The geometry of the domain and the boundary conditions are shown in Fig. 5, and the obtained result in Fig. 6.

4 CONCLUSIONS

In this work, an optimization procedure for the optimal design of folded plates was proposed. The shape function considered was the total potential elastic energy of the structural system. For the structural model, a linear elastic hypothesis was used for the membrane effects, and the thin plate behavior was considered for the bending effects. The computational optimization problem resolution was performed by using FEM and by coupling ANDES and DKT finite elements.

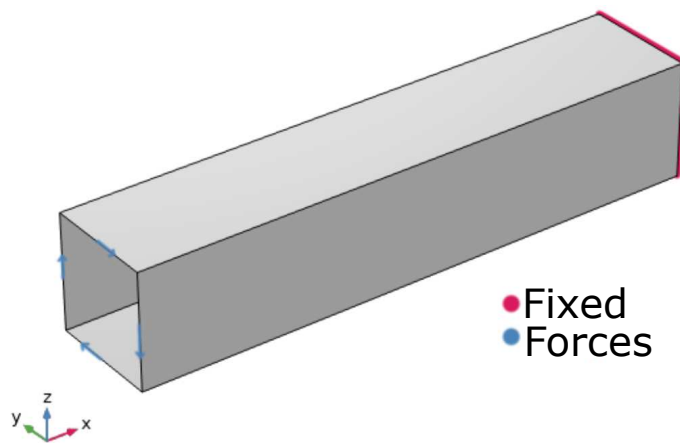


Figure 3: Example 1. Geometry and boundary conditions.

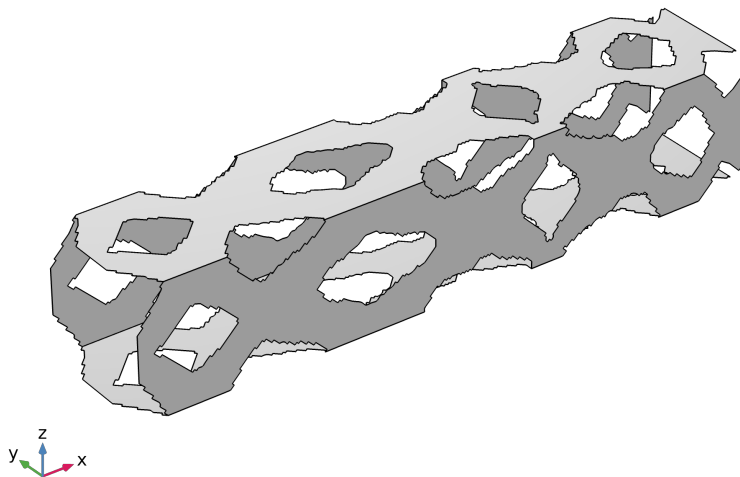


Figure 4: Example 1. Final topology

The topological derivative within the level-set geometrical domain representation was used for the optimization part of the procedure. Since the domain is composed of an arrangement of plates, the kinematics of the membrane and bending effects are decoupled inside the domain of each plate. The coupling comes for the side belonging to two or more plates. We present two numerical realizations showing the capability of the proposed procedure. The obtained results were satisfactory. In example 1, the obtained topology reproduces the classical beam design for global torsional effects. In example 2, the final topology can be considered a discrete version of classical topological optimization for a full solid 3D domain. The plate arrangements are optimized to reproduce a cantilever 3D beam. This indicates that the proposed methodology can be used as a simple prospect for topological optimization of solid domain and shell-like structures.

Finally, in the QR code of Fig. 5, the initial domain and the optimized topologies can be viewed in a web app for a better understanding of the results.

ACKNOWLEDGEMENTS

This research was partially supported by CONICET (National Council for Scientific and Technical Research, Argentina) and PID-UTN (Research and Development Program of the

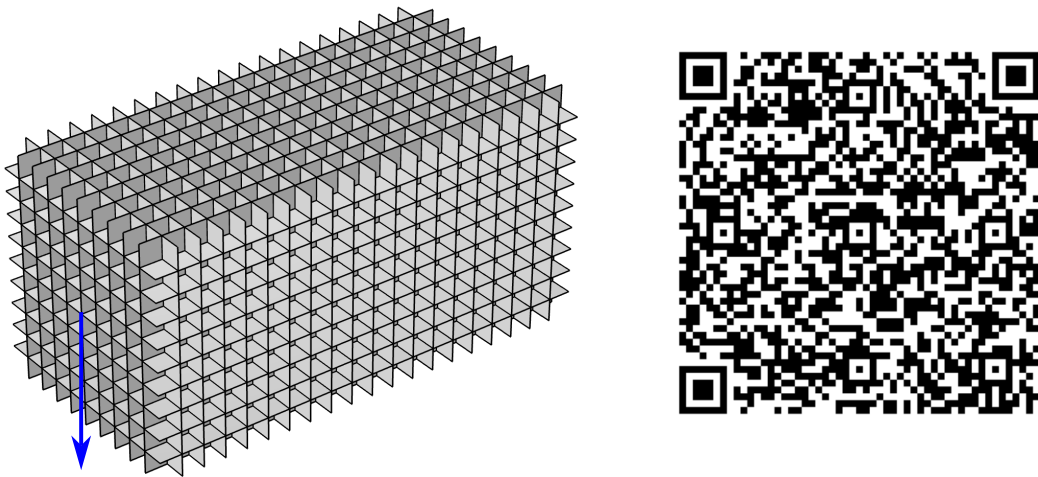


Figure 5: Example 2. Geometry and boundary conditions.

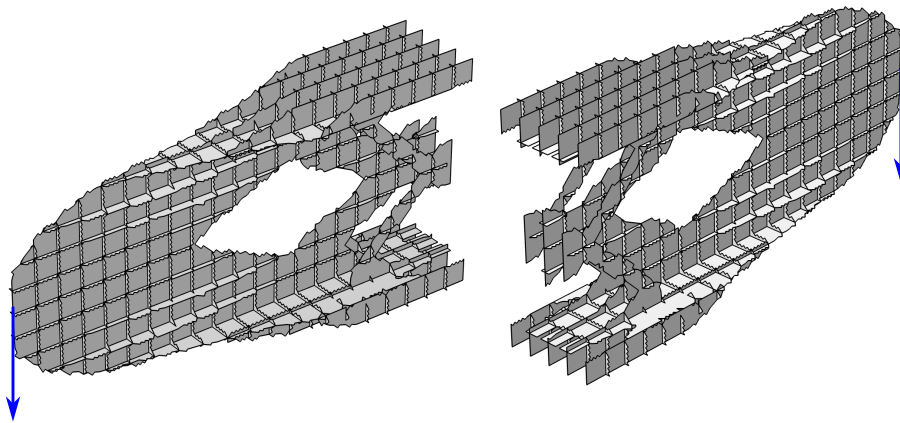


Figure 6: Example 2. Final topology

National Technological University, Argentina). The supports of these agencies are gratefully acknowledged.

REFERENCES

- Amstutz S. A penalty method for topology optimization subject to a pointwise state constraint. *ESAIM: Control, Optimisation and Calculus of Variations*, 16(3):523–544, 2010.
- Amstutz S. and André H. A new algorithm for topology optimization using a level-set method. *Journal of Computational Physics*, 216(2):573–588, 2006.
- Batoz J.L. An explicit formulation for an efficient triangular plate-bending element. *International Journal for Numerical Methods in Engineering*, 18:1077–1089, 1982.
- Campeão D., Giusti S., and Novotny A. Topology design of plates considering different volume control methods. *Engineering Computations*, 31(5):826–842, 2014.
- Carvalho F., Ruschinsky D., Anflor C., Giusti S., and Novotny A. Topological derivative-based topology optimization of plate structures under bending effects. *Structural and Multidisciplinary Optimization*, 63:617–630, 2021. doi:10.1007/s00158-020-02710-4.
- Felippa C. A study of optimal membrane triangles with drilling freedoms. *Computer Methods in Applied Mechanics and Engineering*, 192(16-18):2125–2168, 2003.
- Felippa C. and Militello C. Membrane triangles with corner drilling freedoms-ii. the andes

- element. *Finite Elements In Analysis and Design*, 12(3-4):189–201, 1992.
- Novotny A. and Sokołowski J. *Topological derivatives in shape optimization*. Interaction of Mechanics and Mathematics. Springer-Verlag, Berlin, Heidelberg, 2013. doi: 10.1007/978-3-642-35245-4.
- Romero A. Optimum design of two-material bending plate compliant devices. *Engineering Computations*, 39(1):395–420, 2022.
- Romero A.A. and Giusti S.M. A robust topological derivative-based multi-material optimization approach: Optimality condition and computational algorithm. *Computer Methods in Applied Mechanics and Engineering*, 366:113044, 2020.
- Sales V., Novotny A., and Rivera J.M. Energy change to insertion of inclusions associated with the Reissner-Mindlin plate bending model. *International Journal of Solids and Structures*, 59:132–139, 2015.
- Sokołowski J. and Zolésio J.P. *Introduction to shape optimization - shape sensitivity analysis*. Springer-Verlag, Berlin, Germany, 1992.
- Żochowski A. Optimal perforation design in 2-dimensional elasticity. *Mechanics of Structures and Machines*, 16(1):17–33, 1988.